Measurement of Secondary Gamma-ray Spectra from Structural and Blanket Materials bombarded by D-T Fusion Neutrons

Takashi Nishio[1)], Isao Murata[1)], Akito Takahashi[1)], Fujio Maekawa[2)] and Hiroshi Takeuchi[2)]

1) Department of Nuclear Engineering, Osaka University
Yamada-oka, 2-1, Suita, 565-0871, Japan
e-mail: nishio@newjapan.nucl.eng.osaka-u.ac.jp
2) Japan Atomic Energy Research Institute
Tokai-mura, Ibaraki 319-1195, Japan

Benchmark experiments have been carried out to validate the nuclear data files of JENDL-3.2, JENDL fusion file, ENDF/B-VI, FENDL/E-1.0 and FENDL/E-2.0 for blanket materials of $LiAlO_2$, Li_2TiO_3 and Li_2ZrO_3 and structural materials, i.e., C, V, Fe, SUS-316, Cu, Pb and W at Fusion Neutronics Source (FNS) of JAERI, Japan. Some discrepancies between measured and calculated spectra were observed. However, the C/E values for the energy multiplied integral spectrum show that all the nuclear data files were fairly reliable.

1.Introduction

In a fusion reactor design, neutron reaction cross section data are required and usually the evaluated values in nuclear data files are used for the neutronics calculation. So it is very important to carry out the benchmark experiments for candidate blanket and structural materials and to analyze their results in order to validate the nuclear data. In this study, benchmark experiments have been carried out to validate the nuclear data files of JENDL-3.2, JENDL fusion file, ENDF/B-VI, FENDL/E-1.0 and FENDL/E-2.0 for blanket materials of $LiAlO_2$, Li_2TiO_3 and Li_2ZrO_3 and structural materials, i.e., C, V, Fe, SS316, Cu, Pb and W, at Fusion Neutronics Source (FNS) of JAERI, Japan. The former three are regarded as an advanced solid breeder material because of their inherent advantages such as chemical stability at high temperature, good tritium recovery characteristics and so on, however the experimental data of these blanket materials have not been obtained so far. The latters are well-known important structural materials to be used in a fusion reactor.

2.Experiment

The experiments have been carried out at FNS. Secondary gamma ray spectra from the slab assemblies have been measured using an NaI (Tl) (3"-diam by 3"-long) scintillation detector for three emission angles of 0, 24.9 and 50.0 deg. by using the time-of-flight (TOF) method. The dimensions of the assemblies were 654～2088cm^2 in the front surface (square or circle) and 5.0～40.6cm in thickness as shown in Table 1. Figure 1 shows the experimental arrangement. The detector was positioned at about 7.5m from the slab assembly to realize good energy resolution by the TOF method. The detector was heavily shielded to reduce background gamma rays from other materials except for the sample assembly.

Table 1 Experimental assemblies.

Sample	Shape	Dimensions (cm)
C	Slab	35.6 x 35.6 x t10.2, t25.4, t40.6
V	Slab	25.4 x 25.4 x t10.2, t25.4
Cu	Slab	45.7 x 45.7 x t10.2, t25.4
Pb	Slab	40.0 x 40.0 x t5.0
W	Slab	35.6 x 35.6 x t5.1, t10.2
Fe	Slab	30.0 x 40.0 x t10.0
SS316	Slab	35.6 x 35.6 x t10.2, t20.3
$LiAlO_2$	Slab	25.4 x 25.4 x t10.2, t25.4
Li_2TiO_3	Slab	25.4 x 25.4 x t10.2, t25.4
Li_2ZrO_3	Pseudo-cylinder	23.8φ x t10.2, t25.4

3.Data analysis

The response matrix of the NaI(Tl) scintillation detector was made from the results of the Monte Carlo code MCNP-4B calculation. It was confirmed that the calculated response function agrees well with the measured pulse height spectrum using the standard gamma-ray sources within 10%. The unfolding code HEPRO was used to convert measured pulse height spectrum into energy spectrum. The experimental energy spectra were compared with the calculated results obtained by using the Monte Carlo code MCNP-4B to discuss the validity of the evaluated nuclear data files of JENDL-3.2, JENDL fusion file, FENDL/E-1.0, FENDL/E-2.0 and ENDF/B-VI. Original nuclear data quoted in each nuclear data library for each element are listed in Table 2. The assemblies as well as the detector collimator were modeled precisely for the MCNP calculation. The neutron and gamma-ray source spectrum made and used in FNS was used.

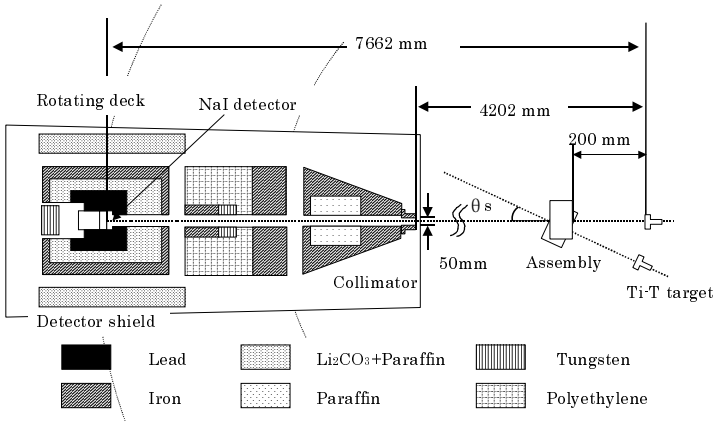

Fig.1 Experimental arrangement.

Table 2 Libraries used in the calculation.

Library name used in the calculation	Nuclear data quoted*1										
	Li	O	Al	Ti	Zr	C	V	Fe	Cu	Pb	W
JENDL-3.2	J32	J32	J32	J32	J32	J32	J32	J32	J32	J32	J32
JENDL-FF	J32	J32	JFF	JFF	JFF	J32	JFF	JFF	JFF	JFF	JFF
ENDF/B-VI	B-VI	B-VI	B-VI	B-VI	B-VI	B-VI	B-VI	B-VI	B-VI	B-VI	BVI
FENDL/E-1.0	B-VI	B-VI	J31	J31	B2	B-VI	B-VI	B-VI	B-VI	B-VI	B-VI
FENDL/E-2.0	B-VI	J32	EF3	J31	JFF	JFF+ B-VI	JFF	B-VI+ EF3	B-VI	B-VI	JFF

*1 J32, JFF, B-VI, J31, EF3 and B2 are abbreviations of JENDL-3.2, JENDL fusion file, ENDF/B-VI, JENDL-3.1, EFF-3 and BROND-2, respectively

4.Results

i) Carbon

Figure 2 shows the comparison of measured and calculated gamma-ray spectra for carbon of 10.16 cm in thickness and scattering angle of 50.0 degree. The calculated spectra are in almost good agreement with all the experimental data for all the nuclear data files.

ii) Vanadium

Figure 3 shows the comparison of measured and calculated gamma-ray spectra for vanadium of 10.16 cm in thickness and scattering angle of 24.9 degree. All the calculated spectra show underestimation leading to the conclusion that the evaluated secondary gamma ray production cross sections may be small. The peaks around 1.5 and 3 MeV are not reproduced in all the nuclear data files.

iii) Iron

Figures 4 and 5 show the comparison of measured and calculated gamma-ray spectra for iron of 10.16 cm in thickness and scattering angle of 50.0 degree and the evaluated gamma ray emission energy differential cross section (EDX) of ^{nat}Fe, respectively. JENDL fusion file is in fairly good agreement with the experimental data as shown in Fig. 4. Overestimation of the secondary gamma ray production cross section in JENDL-3.2 is reconfirmed [1]. The cross section of ^{56}Fe in ENDF/B-VI is adopted in FENDL/E-1.0, also that of ^{56}Fe in EFF-3 is adopted in FENDL/E-2.0 as shown in Table 2. As a result, the peak of 1238 keV from ^{56}Fe has not been reproduced in FENDL/E-2.0 as one can see it from the EDX spectrum of ^{56}Fe,though the reproduction is fairly good in FENDL/E-1.0.

iv) SS316

Figure 6 shows the comparison of measured and calculated gamma-ray spectra for SS316 of 10.16 cm in thickness and scattering angle of 50.0 degree. The result shows the same tendency as the case of iron because SS316 is mainly composed of iron. The influences of other elements such as Ni and Mn were not observed.

v) Copper

Figure 7 shows the comparison of measured and calculated gamma-ray spectra for copper of 10.16 cm in thickness and scattering angle of 50.0 degree. Large discrepancy is not observed and five nuclear data files reproduce the measured spectrum very well. Five nuclear data files are therefore confirmed to be fairly reliable with respect to the prediction of gamma ray spectrum.

vi) Lead

Figures 8 and 9 show the comparison of measured and calculated gamma-ray spectra for lead of 5.00 cm in thickness and scattering angle of 50.0 degree and the evaluated gamma ray emission EDX of ^{nat}Pb, respectively. ENDF/B-VI calculation gives the best agreement with the experimental data among five nuclear data files. In JENDL-3.2 and JENDL fusion file, the peaks of 1770 keV and 2615 keV from ^{nat}Pb are not observed because there is no structure around 2-3 MeV in the EDX spectrum of ^{nat}Pb as shown in Fig. 9.

vii) Tungsten

Figure 10 shows the comparison of measured and calculated gamma-ray spectra for tungsten of 5.08 cm in thickness and scattering angle of 24.9 degree. Because there is no complicated structure including discrete peaks, large discrepancy is not observed, however a slight discrepancy is found around 2 MeV.

viii) $LiAlO_2$

Figures 11 and 12 show the comparison of measured and calculated gamma-ray spectra for $LiAlO_2$ of 25.4 cm in thickness and scattering angle of 24.9 degree and the evaluated gamma ray emission EDX of ^{nat}O, respectively. A significant discrepancy between the experimental and calculated spectra is observed around 6 MeV in JENDL-3.2 and JENDL fusion file as shown in Fig. 11, that is due to the fact that the intensity of the 6130 keV gamma ray from the second excited level of ^{16}O is not evaluated in JENDL-3.2 and JENDL fusion file as shown in the EDX spectrum of Fig. 12. All the nuclear data files properly reproduce discrete gamma ray peaks from ^{27}Al.

ix) Li_2TiO_3

Figures 13 and 14 show the comparison of measured and calculated gamma-ray spectra for Li_2TiO_3 of 10.16 cm in thickness and scattering angle of 50.0 degree and the evaluated gamma ray emission EDX of ^{nat}Ti, respectively. The same tendency as $LiAlO_2$ is observed for ^{16}O. The calculated spectra in JENDL-3.2 and JENDL fusion file agree well with the experimental data below 3 MeV as shown in Fig.13. The ENDF/B-VI calculation seems to underestimate expcept for peaks over 5 MeV as is understood from the EDX spectrum of ^{nat}Ti in Fig.14.

x) Li_2ZrO_3

Figures 15 and 16 show the comparison of measured spectra and calculated gamma-ray spectra for Li_2ZrO_3 of 10.16 cm in thickness and scattering angle of 24.9 degree and the measured gamma ray spectrum of ^{nat}Zr with Hp-Ge detector by Kondo et. al.[2], respectively. A large underestimation is observed for ENDF/B-VI as shown in Fig.15 because there is no evaluated secondary gamma ray production cross section for Zr. The FENDL/E-1.0 calculation is in excellent agreement with the experimental data among all the nuclear data files. This means that the secondary gamma ray production cross section of ^{nat}Zr in BROND-2 is very reliable. The gamma ray peak around 2 MeV from ^{nat}Zr is not reproduced in all the nuclear data files, though this peak was observed in the measured gamma ray spectrum as shown in Fig.16.

xi) The ratio of C/E in energy integral

The ratio of calculated to measured gamma ray spectrum multiplied by the gamma ray energy (C/E) is described for all the samples in Fig.17. The C/E values deviate within $\pm$ 20% from 1.0 except for ^{nat}V and ^{nat}Fe. All the nuclear data files are thus confirmed to be reliable in general with respect to the prediction of gamma ray transport.

5.Conclusion

Secondary gamma ray benchmark experiments for advanced blankets and structural materials have been conducted. The nuclear data files of JENDL-3.2, JENDL fusion file, ENDF/B-VI, FENDL/E-1.0 and FENDL/E-2.0 were validated by means of comparing measured with calculated secondary gamma ray spectra. It was found from the comparison that there were some discrepancies between experiment and calculation and it was pointed out that several nuclear data files should be improved. However, for the energy integral, all the C/E values deviate within 20% except for ^{nat}V and ^{nat}Fe in all the nuclear data files.

Acknowledgments

The authors wish to acknowledge the operating staff of FNS, JEARI. for their excellent operation of FNS.

Reference

[1] Maekawa F., Oyama Y., Konno C., Wada M. and Ikeda Y.: Nucl. Sci. Eng., 126, 187 (1997).
[2] Kondo T. Private Communication, Osaka University (1999).

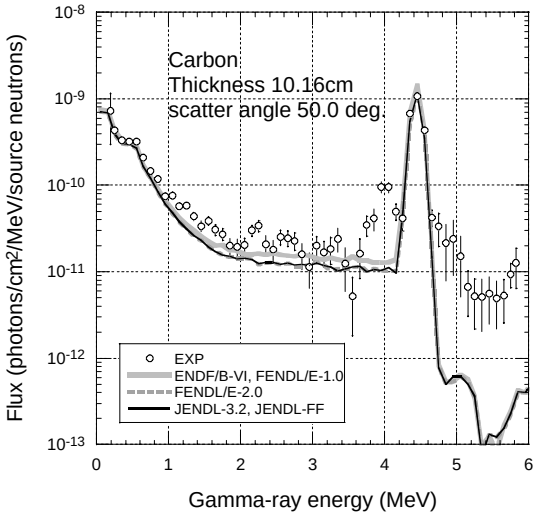

Fig.2 Gamma-ray flux for Carbon of 10.16 cm in thickness at 50.0 degree

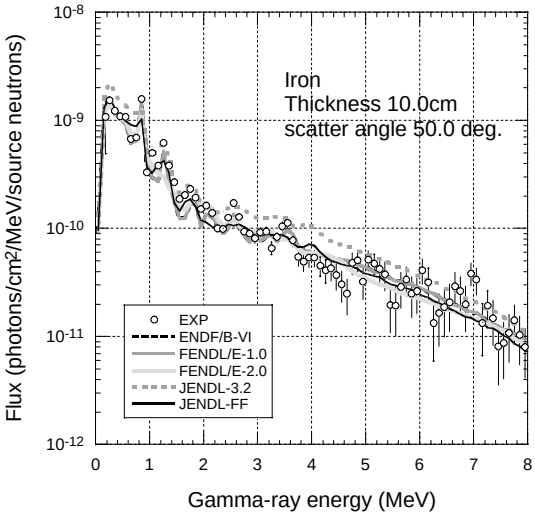

Fig.4 Gamma-ray flux for Iron of 10.16 cm in thickness at 50.0 degree

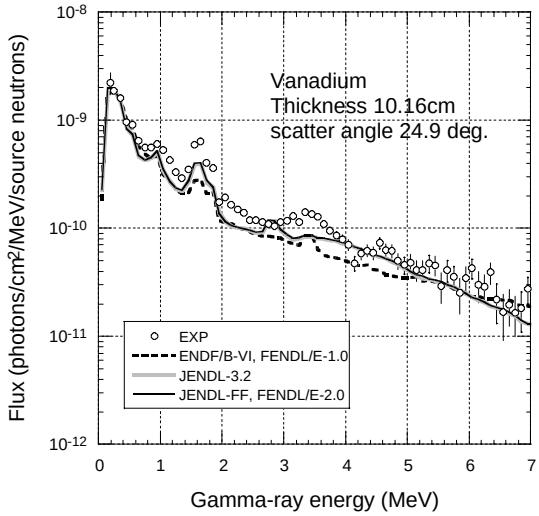

Fig.3 Gamma-ray flux for Vanadium of 10.16 cm in thickness at 24.9 degree

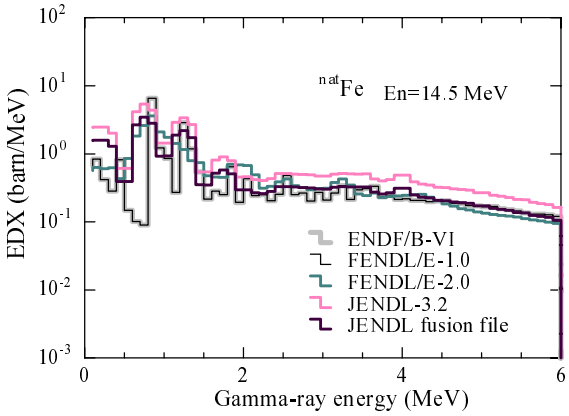

Fig.5 Evaluated gamma ray emission EDX of ^{nat}Fe

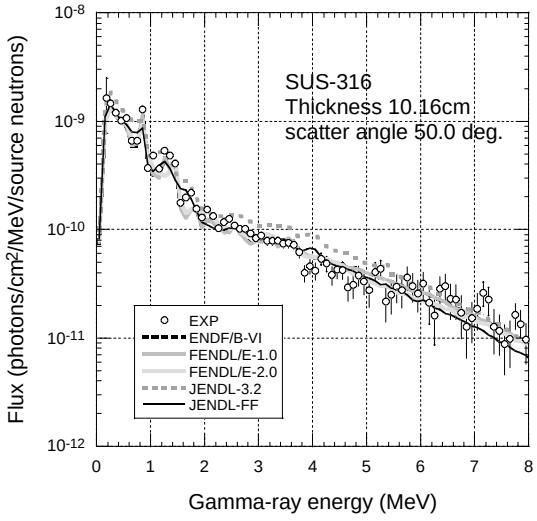

Fig.6 Gamma-ray flux for SUS-316 of 10.16 cm in thickness at 50.0 degree

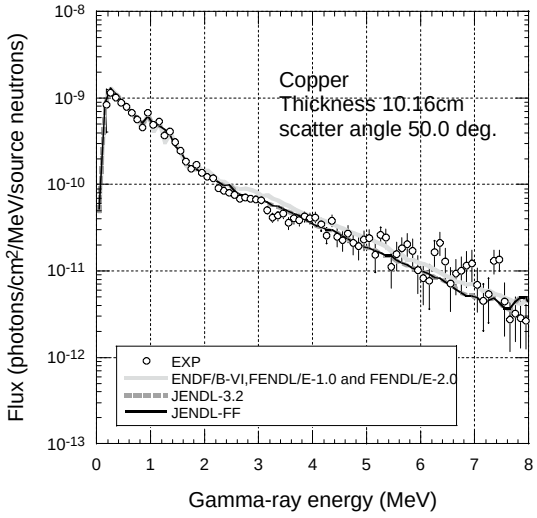

Fig.7 Gamma-ray flux for Copper of 10.16 cm in thickness at 50.0 degree

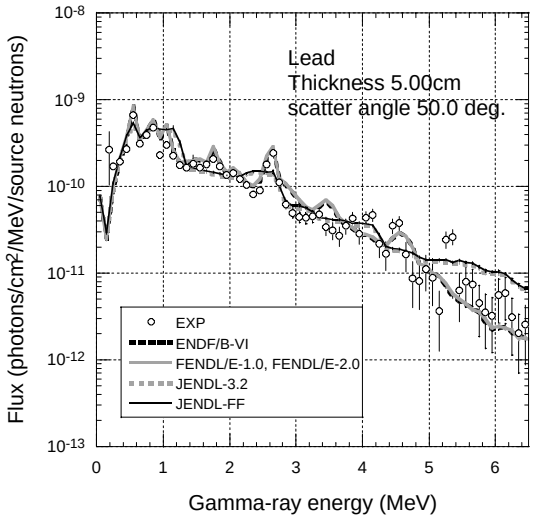

Fig.8 Gamma-ray flux for Lead of 5.00 cm in thickness at 50.0 degree

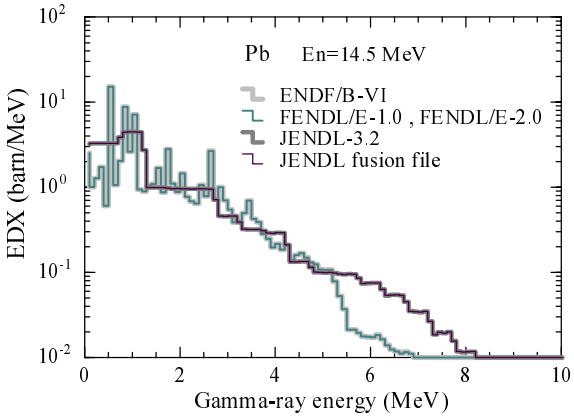

Fig.9 Evaluated gamma ray emission EDX of ^{nat}Pb

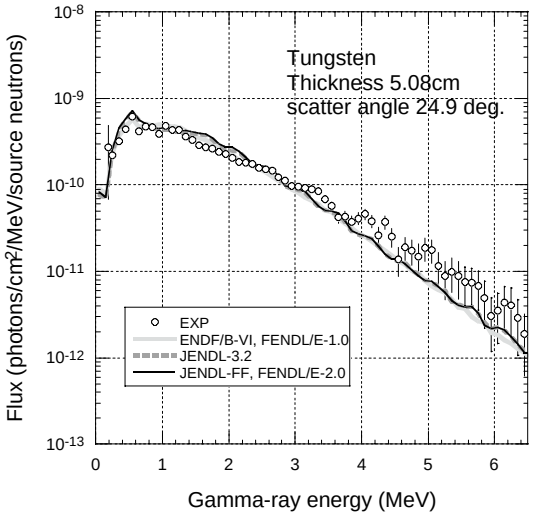

Fig.10 Gamma-ray flux for Tungsten of 5.08 cm in thickness at 24.9 degree

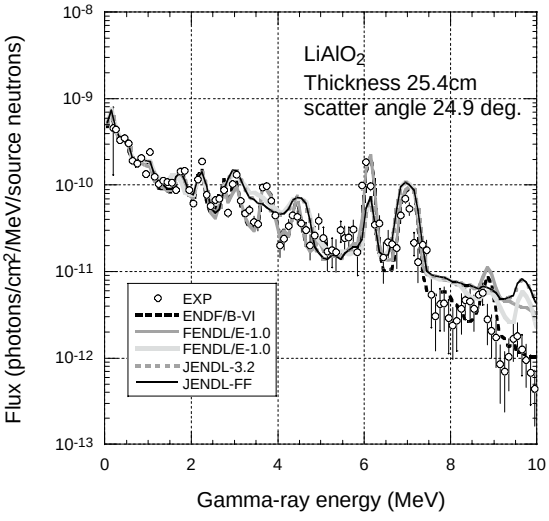

Fig.11 Gamma-ray flux for $LiAlO_2$ of 25.4 cm in thickness at 24.9 degree

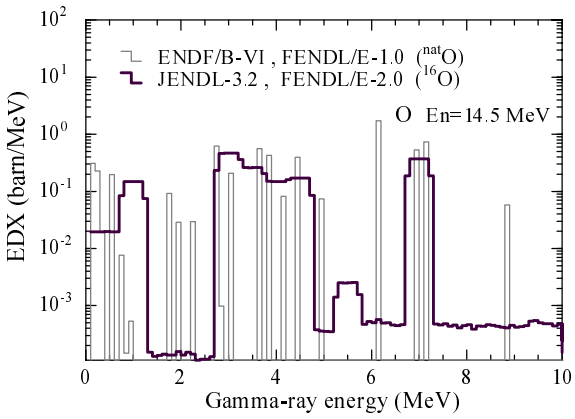

Fig.12 Evaluated gamma ray emission EDX of ^{nat}O

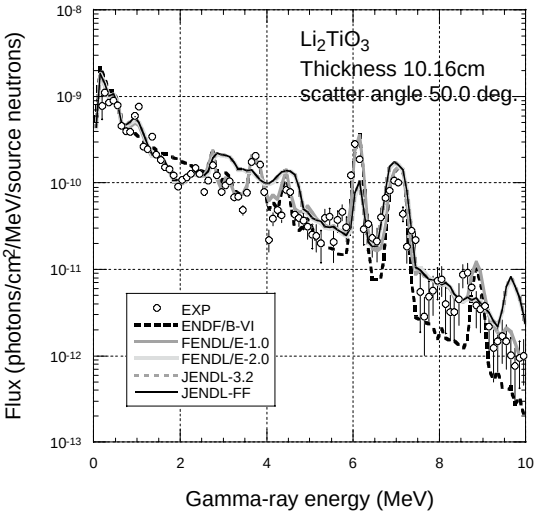

Fig.13 Gamma-ray flux for Li_2TiO_3 of 10.16 cm in thickness at 50.0 degree

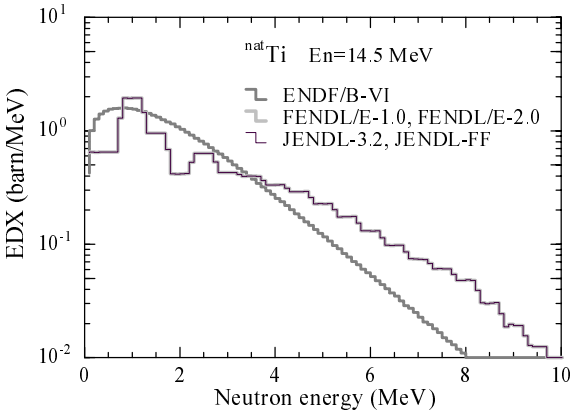

Fig.14 Evaluated gamma ray emission EDX of ^{nat}Ti

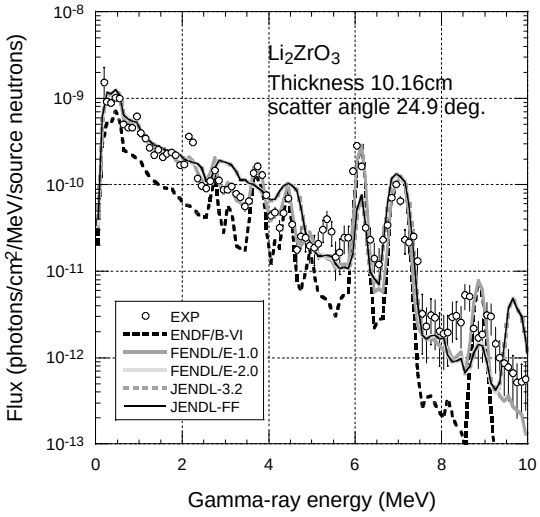

Fig.15 Gamma-ray flux for Li_2ZrO_3 of 10.16 cm

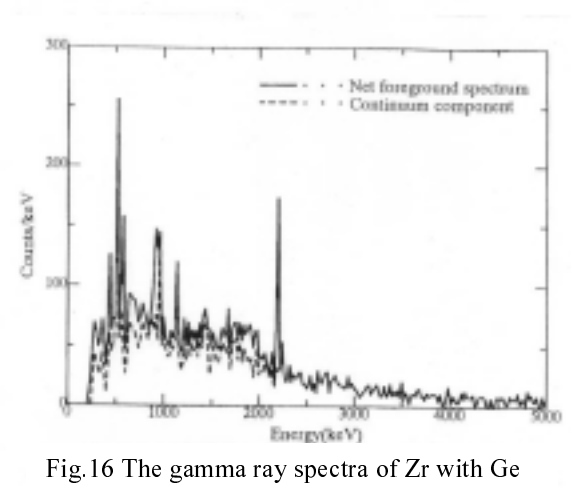

Fig.16 The gamma ray spectra of Zr with Ge detector by Kondo et. al.

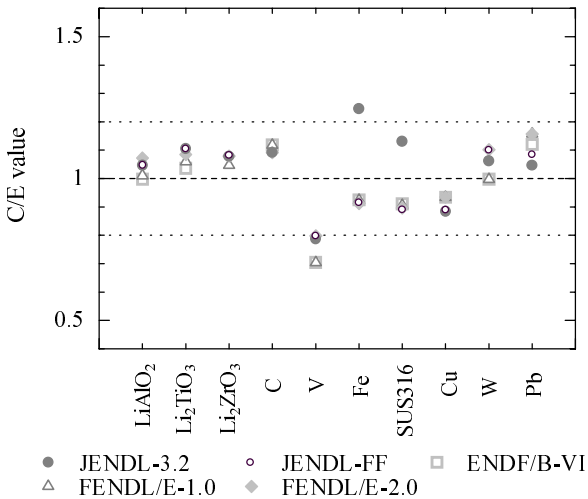

Fig.17 The ratio of calculation to experiment